Supporting Information

Peptide-Carbon Hybrid Membranes for Highly Efficient and Selective Extraction of Actinides from Rare Earth Elements

Yangyang Gao,[a] Qian Zhang,[a] Ying Lv,[b] Sheng Wang,[a] Meng Men,[c] Hisayoshi Kobayashi,[d] Zhanglian Xu,[a] Yin Wang*[e]*

a. *Shaanxi Key Laboratory of Advanced Nuclear Energy and Technology and Shaanxi Engineering Research Center of Advanced Nuclear Energy, School of Nuclear Science and Technology, Xi'an Jiaotong University, Xi'an, Shaanxi, 710049, P. R. China.*
E-mail: xuzhanglian@xjtu.edu.cn
b. *College of Materials Science and Engineering, Xi'an Shiyou University, No.18, 2nd East Dianzi Road, Xi'an, Shaanxi, 710065, P. R. China*
c. *Shaanxi Province Radioactive Environmental Supervision and Management Station, Xi'an, Shaanxi, 710065, P. R. China*
d. *Emeritus professor of Kyoto Institute of Technology, Matsugasaju, Sakyo-ku, Kyoto, 606-8585, Japan*
e. *School of Pharmacy, Shanghai Jiao Tong University, Shanghai 200240, P. R. China; Department of Chemistry and Macromolecules Innovation Institute, Virginia Tech, Blacksburg, VA 24061, United States*
E-mail: yinwang@sjtu.edu.cn or ywang300@vt.edu

Data

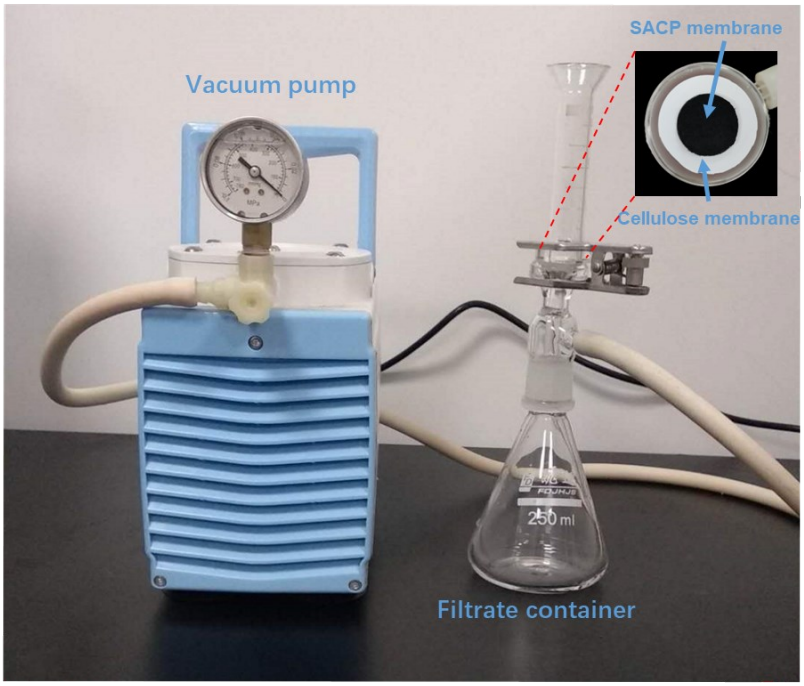

Fig. S1. The photograph of vacuum filtration using in membrane fabrication and pressure-driven adsorption.

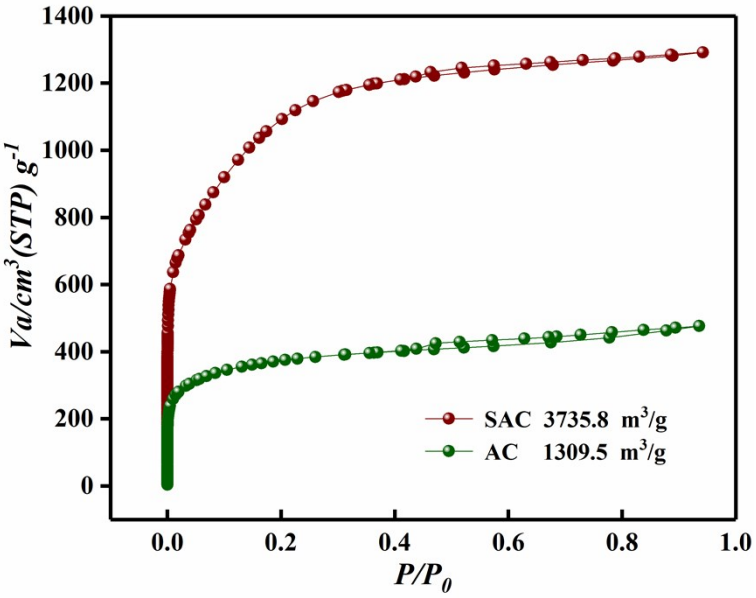

Fig. S2. The nitrogen sorption isotherms of SAC and AC composites.

First, the purity of the peptide was determined by high performance liquid chromatography (HLCP, DGU-20A5R with a LC-20AT infusion pump). As shown in Fig. S3a, a distinct peak

appeared at 17.36 min with 95.69% of the total peak area, indicating the high purity of the peptide produced. Further calculations based on mass spectrometry (MS, Shimadzu LCMC-2020) showed that the relative molecular mass of the peptide was 1359.60 (Fig. S3b), which was very close to its theoretical value of 1359.62, indicating that the designed peptide was successfully prepared.

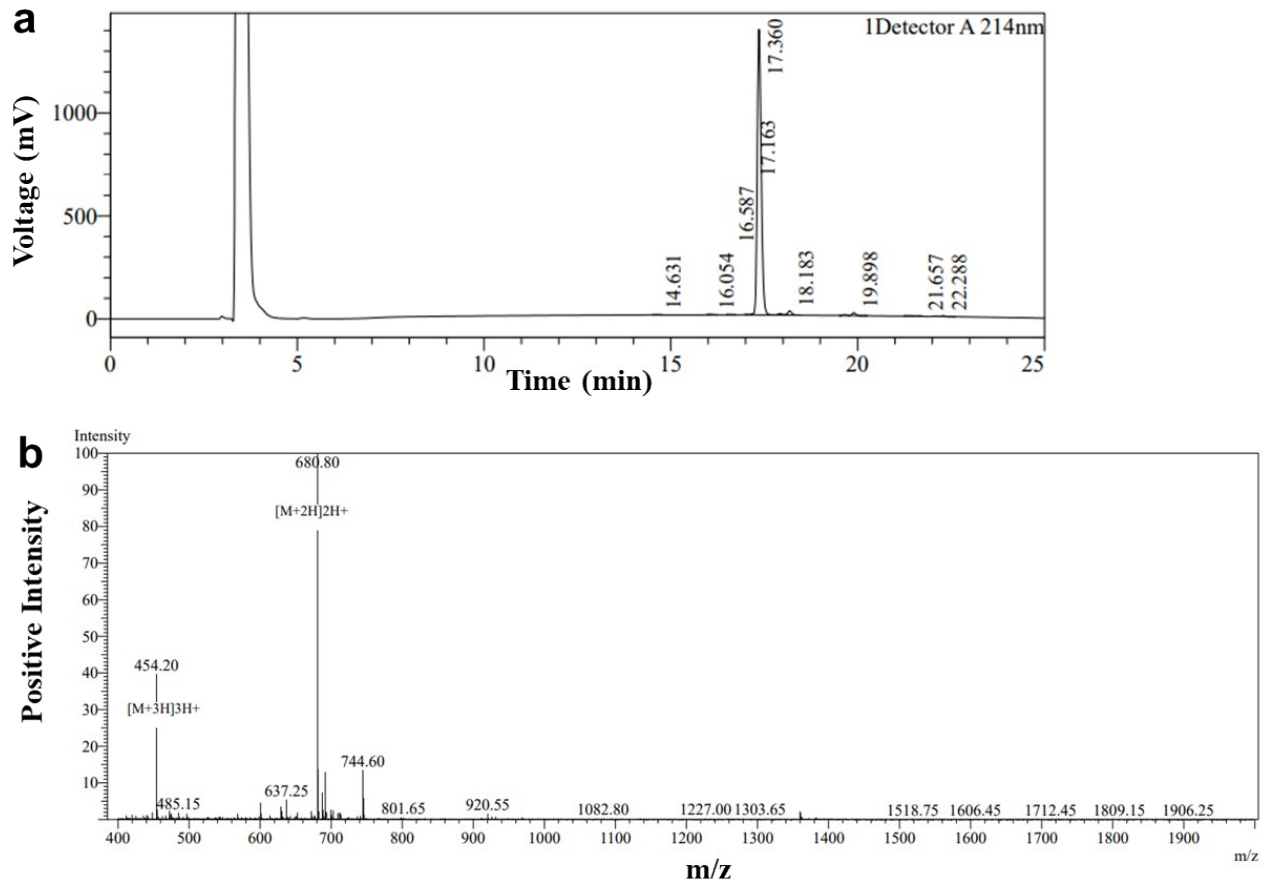

Fig. S3. HPLC and MS characterizations of peptides used in this study.

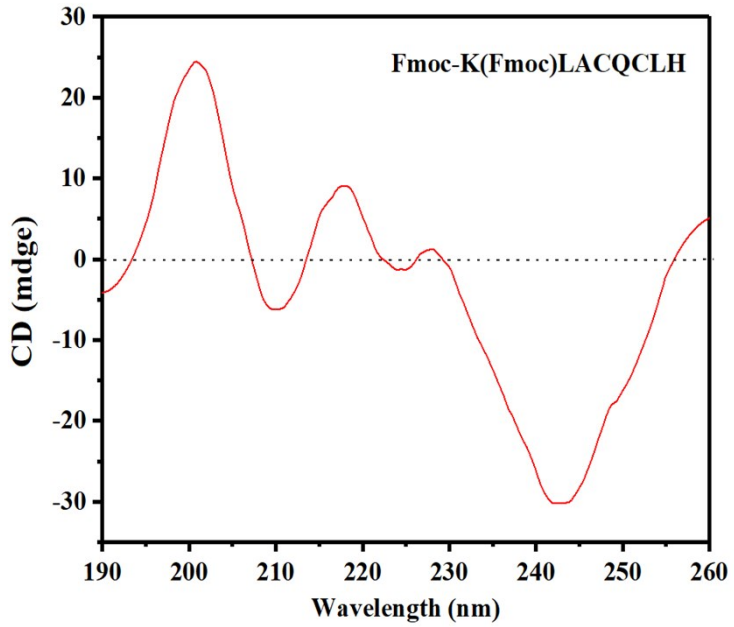

Fig. S4. CD spectrum of rationally designed peptide used in the present study in water/acetonitrile (3:1 v/v) solution.

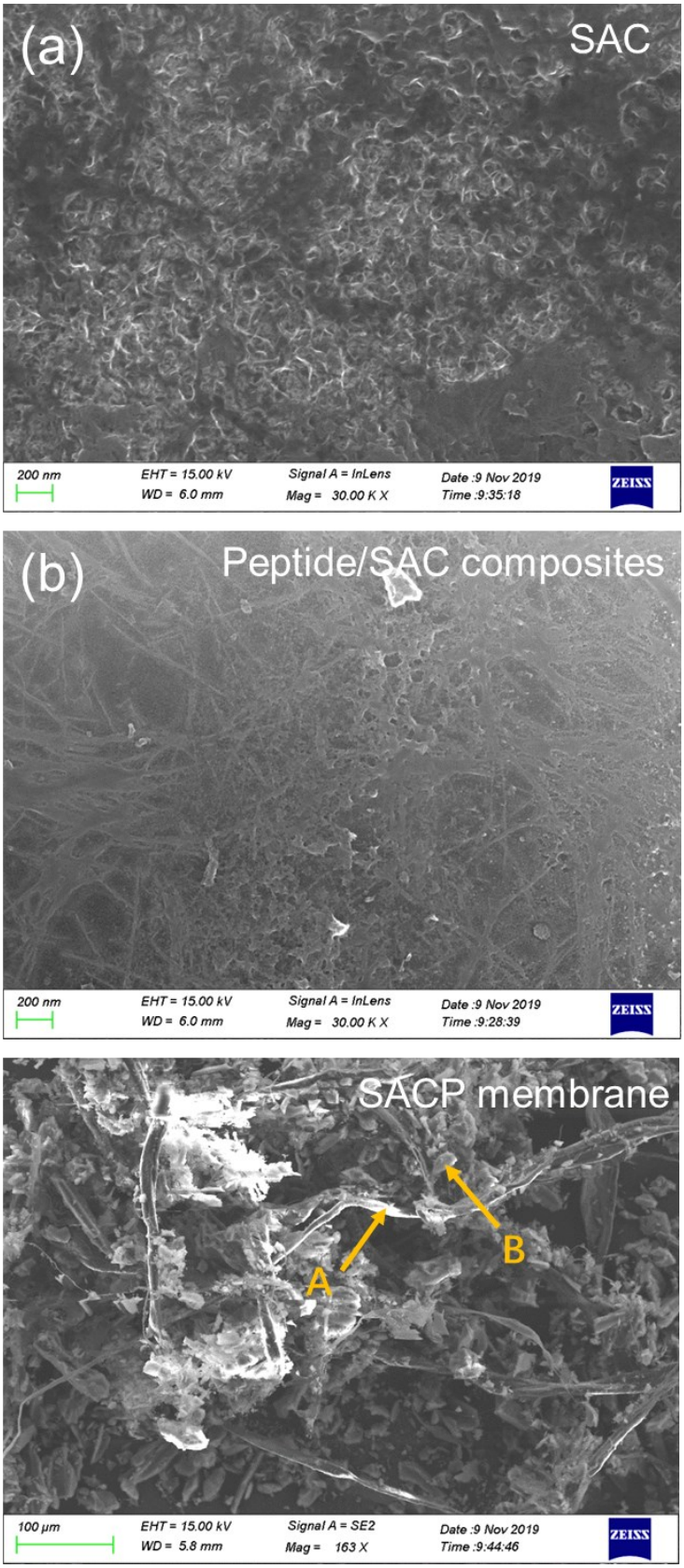

Fig. S5 Representative SEM images of (a) SAC, (b) peptide/SAC composites, and (c) SACP-5 membrane, arrows A and B represent paper pulp fiber and peptide/SAC composites, respectively.

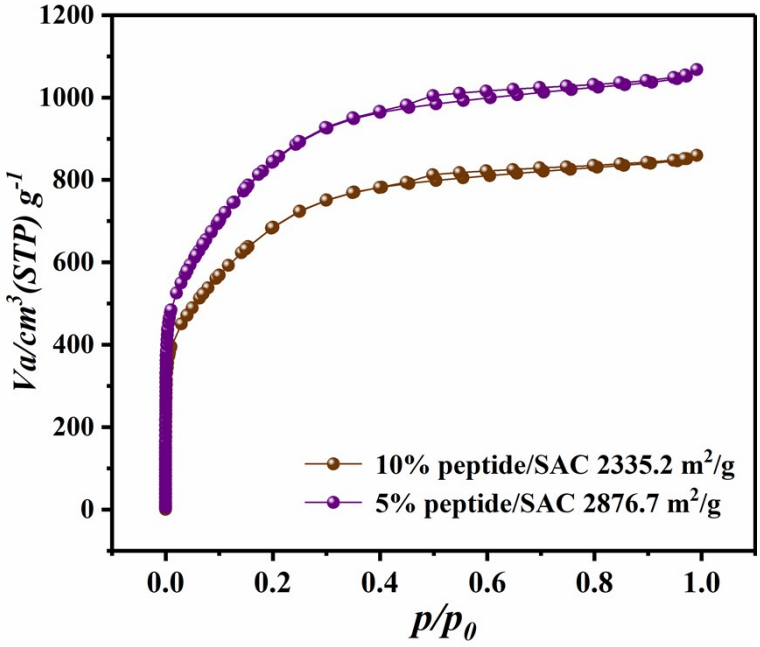

Fig. S6 The nitrogen sorption isotherms of 5% and 10% peptide/SAC composites.

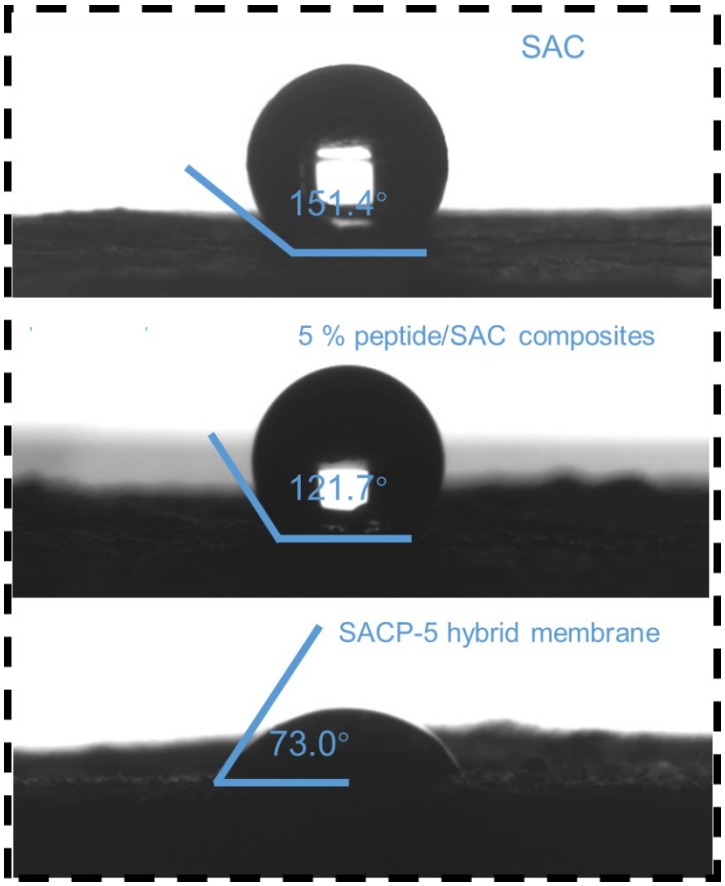

Fig. S7 Water contact angle images of SAC, 5% peptide/SAC composites, and the SACP-5 hybrid membranes.

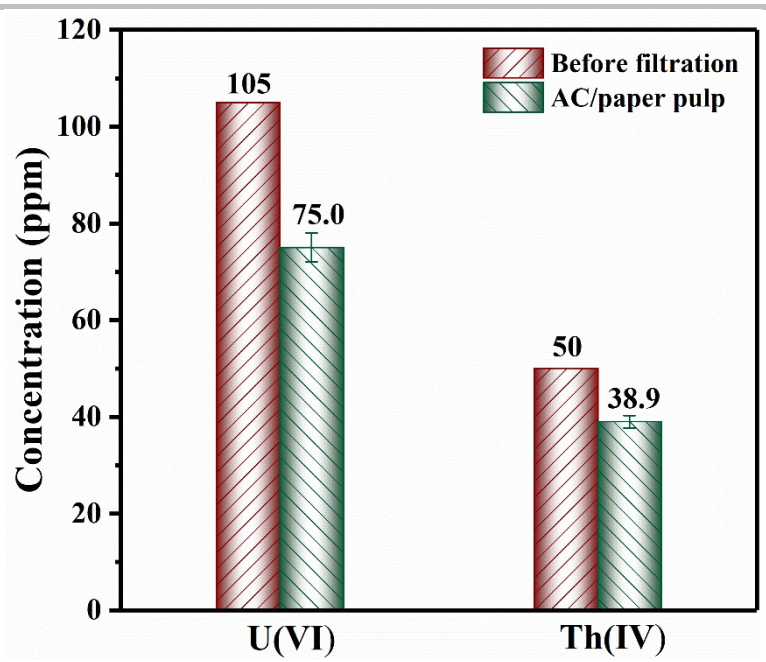

Fig. S8 Removal performance of AC membranes for U(VI) and Th(IV), pH values of U(VI) and Th(IV) solutions were 6.0 and 4.0, respectively.

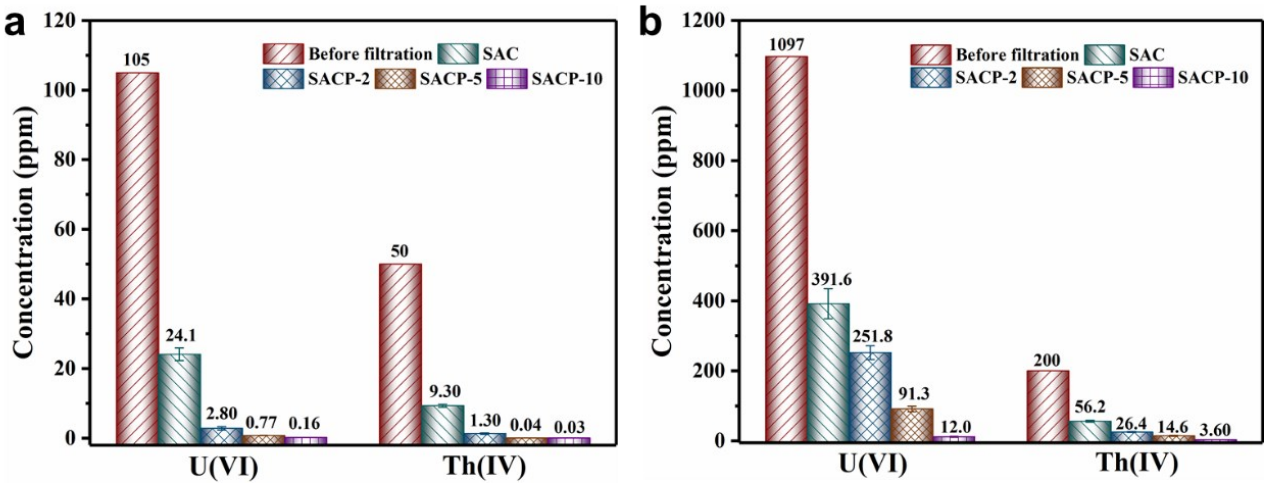

Fig. S9 The filtration performance of the SACP hybrid membranes with different peptide contents. All error bars represent standard deviation from bipartite experiments. The pHs of U(VI) and Th(IV) solutions were 6.0 and 4.0, respectively.

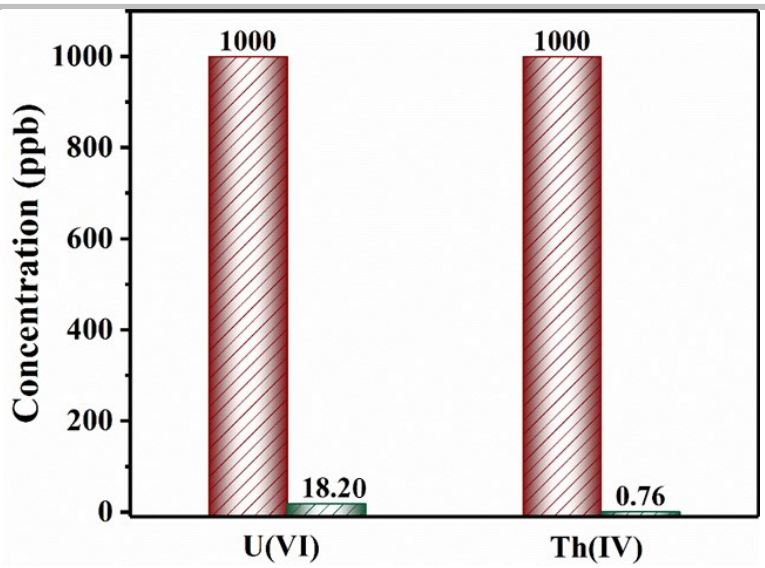

Fig. S10 Filtration performances of the SACP-5 hybrid membranes in removal of U(VI) and Th(IV) at the ultralow concentration of 1000 ppb. The pH values for U(VI) and Th(IV) were 6.0 and 5.0, respectively.

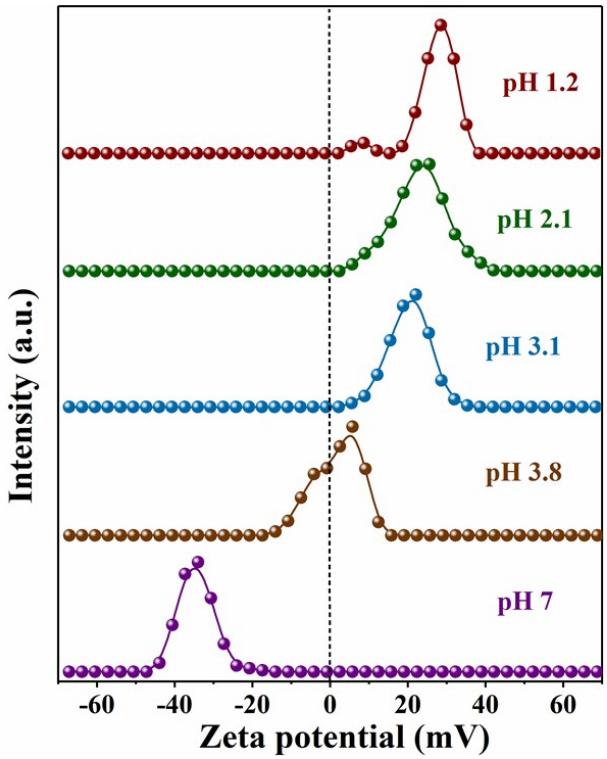

Fig. S11 Zeta potential of SACP-5 at different pHs.

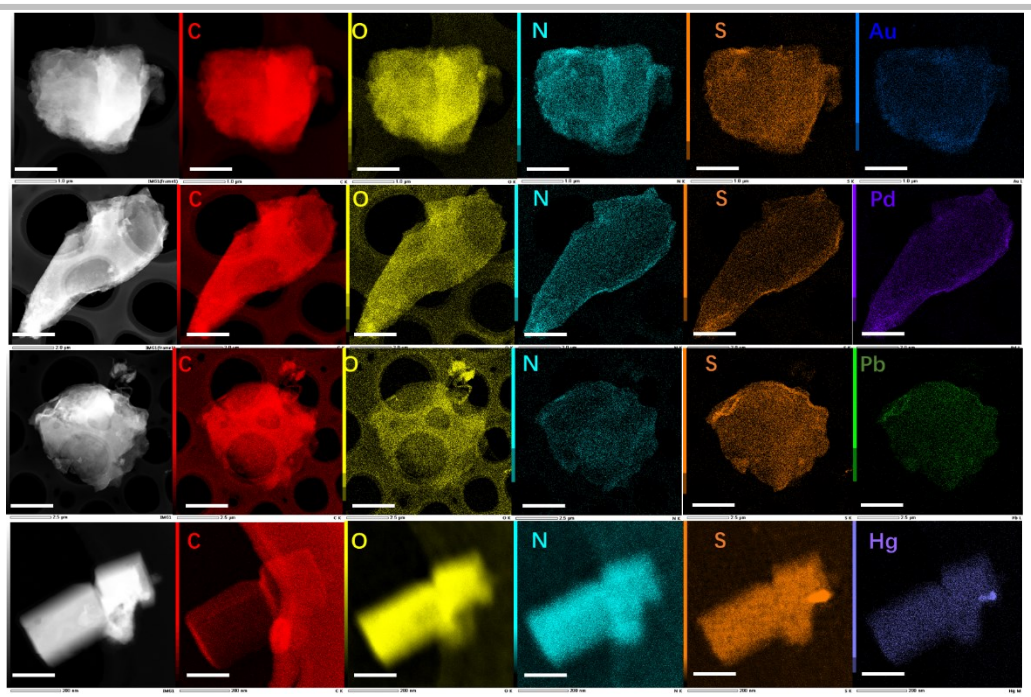

Fig. S12. STEM and elemental mapping images of 5% peptide/SAC composites after adsorbing four HMIs. The scale bars are 1 μm, 2.0 μm, 2.5 μm, and 200 nm for $Au(CN)_2^-$, $PdCl_4^{2-}$, Pb^{2+}, and Hg^{2+}, respectively**.**

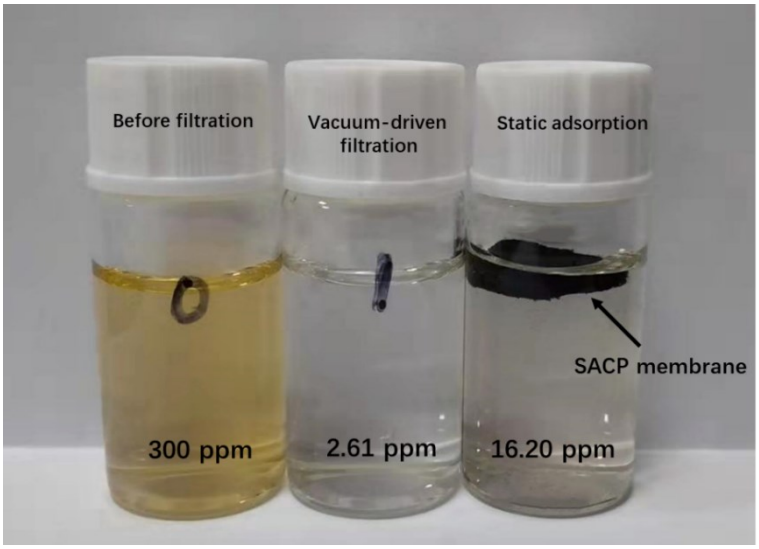

Fig. S13. Adsorption comparison of $PdCl_4^{2-}$ between vacuum-driven filtration (within 1 min) and static adsorption (24 h).

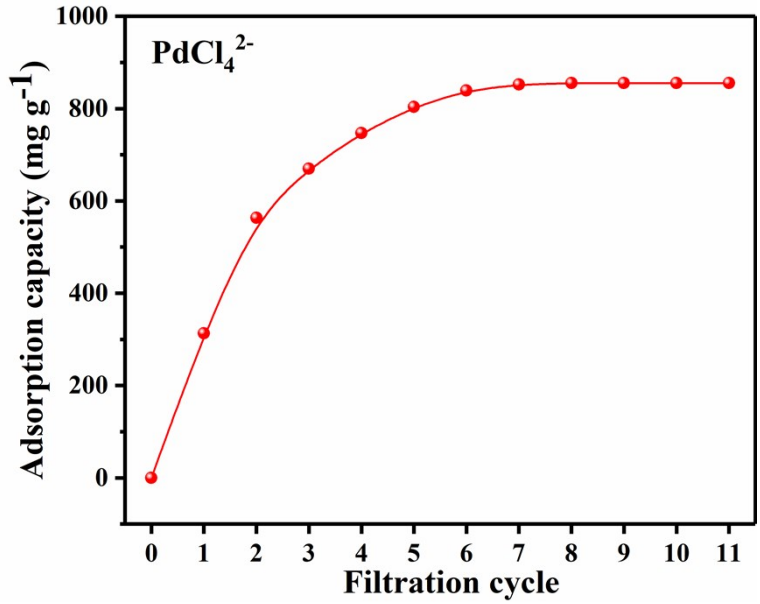

Fig. S14. Saturation adsorption capacity of SACP-5 hybrid membranes for $PdCl_4^{2-}$ (C_0=1000 ppm, pH 1.0).

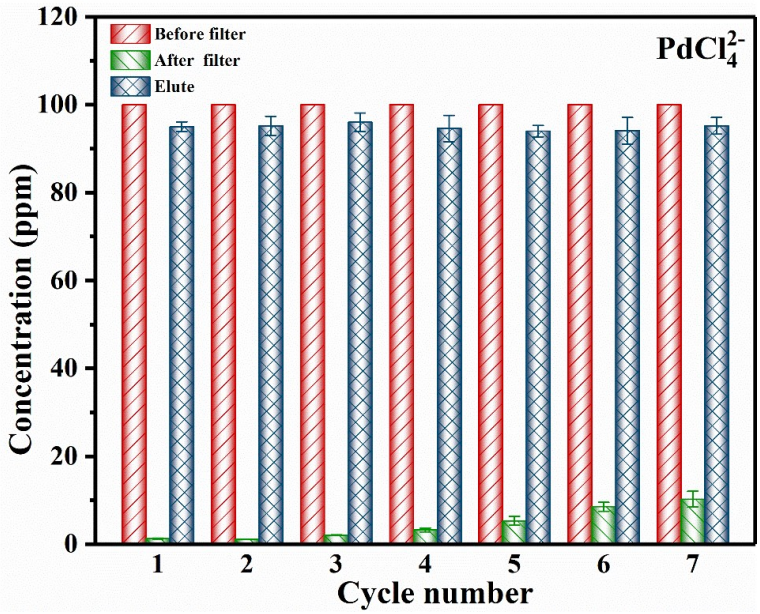

Fig. S15. Reusability of SACP-5 hybrid membranes for $PdCl_4^{2-}$ with 2 wt % EDTA solution as the eluent after each filtration.

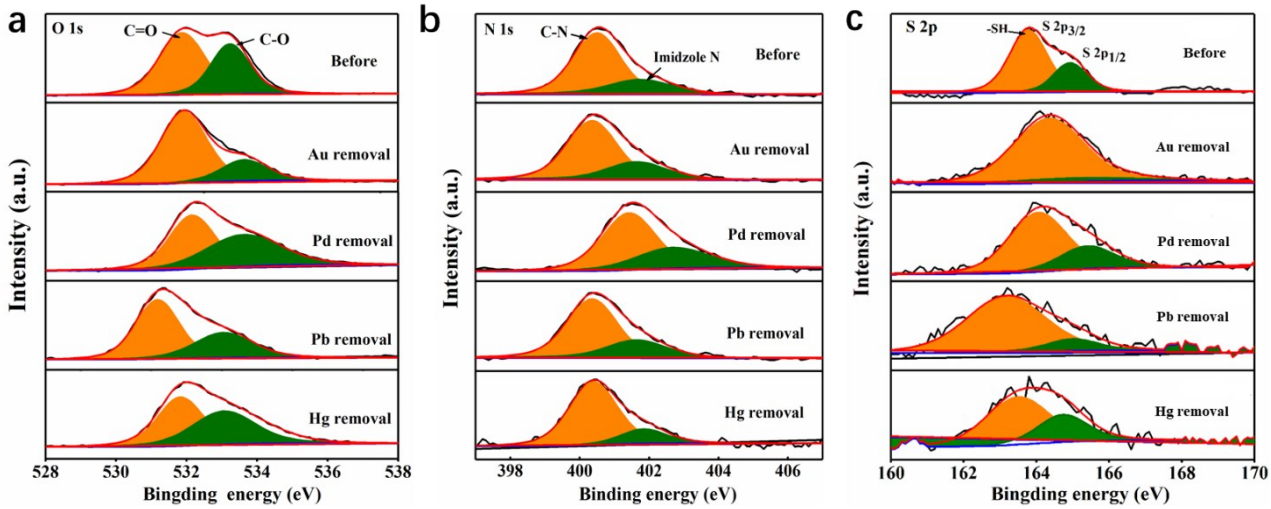

Fig. S16. High-resolution XPS spectra of a) O 1s, b) N 1s, and c) S 2p region of 5% peptide/SAC composites before and after the removal of $Au(CN)_2^-$, $PdCl_4^{2-}$, Pb^{2+}, and Hg^{2+}.

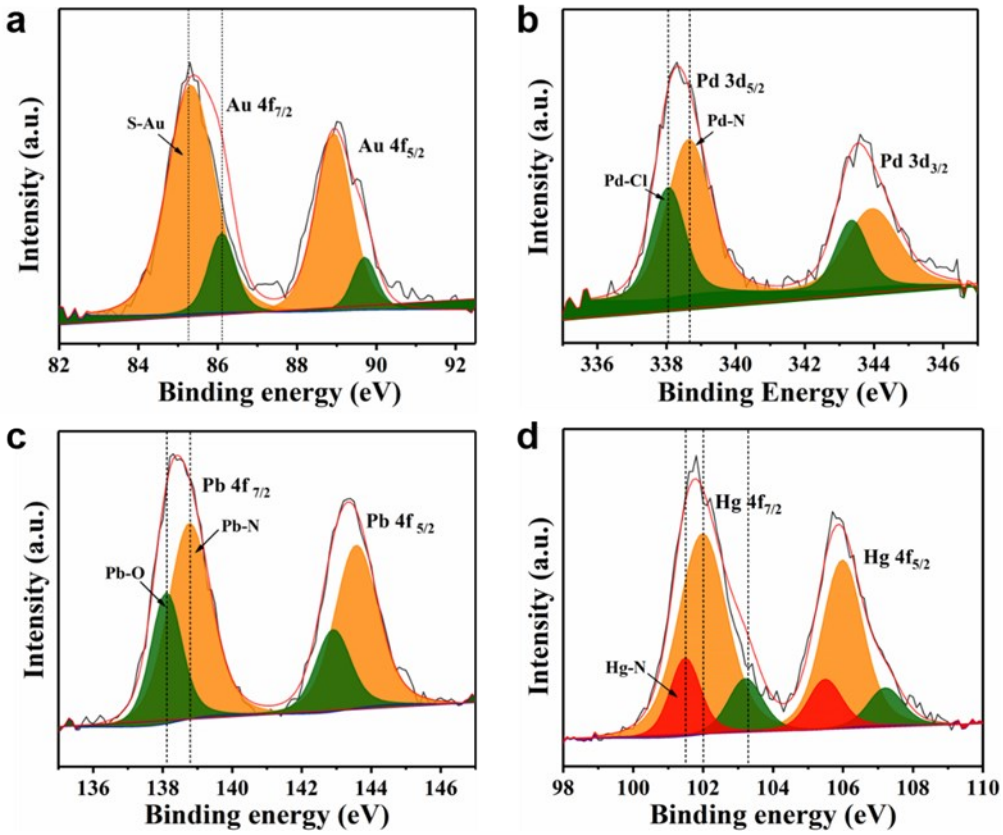

Fig. S17. High-resolution XPS spectra of a) Au 4f, b) Pd 3d, c) Pb 4f, and d) Hg 4f.

Table S1. The constitution of peptide-carbon membranes used in this work.

Membrane	Carbon (mg)	Peptide(mg)	Paper pulp
SAC	30.0 (SAC)	0	15
Peptide	0	1.5	15
SACP-2	29.4 (SAC)	0.6	15
SACP-5	28.5 (SAC)	1.5	15
SACP-10	27.0 (SAC)	3.0	15
AC	30.0 (AC)	0	15

Table S2. The surface area and porosity of different porous carbon materials.

Carbon materials	S_{BET}(m^2 g^{-1})	V_p(cm^3 g^{-1})	Ref
SACP-5	2876.5	1.65	
SACP-10	2335.2	1.33	This study
SAC	3735.8	2.0	
uGil-900	4200	2.41	1
MPPy- derived carbon	4000	3.0	2
CNT composites	1479–3802	0.83-2.98	3
CA-4800	3771	1.75	4
Ac8-CA	3343	2.65	5
ZTC-X	3332	1.66	5
CT-2-800	3010	1.57	4
CA-4900	2864	1.32	4
PFA+propylenes	2170-3600	0.9-1.5	6
Propylene	2260	1.11	6
CA-4700	2001	0.95	4
WMC-O	1056	NA	7
Ordered mesoporous carbons	115-185	1.12-1.63	8

Table S3. K_d values of REEs in the adsorption of SACP-5 for RREs mixed solution without U(VI) and Th(IV).

Elements	K_d (mL g^{-1})
Y	15.71
La	109.34
Ce	5.76
Pr	79.21
Nd	91.30
Eu	94.02
Gd	214.91
Yb	138.14

Table S4. Comparison of absorbents for adsorption time and K_d values.

Absorbents	adsorption time (min)	K_d^U (mL g^{-1})	K_d^{Th} (mL g^{-1})	Ref.
SACP-5 membrane	1 (min/filtration)	5.01×10^7	1.67×10^8	**This study**
Hfp-0.80	120	1.26×10^5	5.84×10^4	9
SiO_2-MeO-2	360	1.9×10^4	9×10^5	10
DVB-VPA	180	NA	NA	11
WMC-O	240	NA	1.3×10^5	7
FJSM-GAS-1	1740	6.06×10^6	NA	12
FJSM-GAS-2	NA	5.12×10^4	NA	12
ACFs-AO	2880	1.99×10^4	NA	13
mGO-PAO	100	4.44×10^5	NA	14
HCPP	180	2.68×10^5	NA	15
P-Fe-CMK-3	30	1×10^5	NA	16
SBA-15-O-DMPA	120	NA	2.0×10^4	17

Movie S1 The SACP-5 hybrid membrane was rigorously stirred without any damage, demonstrating the good mechanical property of this hybrid membrane. **Movie S2** and **Movie S3** show the filtration tests using the SACP-5 hybrid membrane and 5% peptide/SAC composites, respectively. The paper pulp can fix the peptide/SAC composites well thus result in clear filter solution (See Movie S2), while the original peptide/SAC composites without paper pulp suspended into the filtering solution and cannot form the self-standing membranes through vacuum filtration (See Movie S3). Meanwhile, the addition of paper pulp also resulted in the faster filtration kinetics. The pure water flux was improved from 2.14×10^4 L m^{-2} h^{-1} bar^{-1} of peptide/SAC composites to 5.14×10^4 L m^{-2} h^{-1} bar^{-1} of SACP-5 hybrids membrane. (Movie S2 vs Movie S3).

References

1 A. S. Jalilov, Y. Li, J. Tian, J. M. Tour, *Adv. Energy. Mater.* 2017, *7*, 1600693-1600699.
2 B. Adeniran, R. Mokaya, *Nano Energy.* 2015, **16**, 173-185.
3 B. Adeniran, R. Mokaya, *J. Mater. Chem. A.* 2015, **3**, 5148-5161.
4 T. S. Blankenship, N. Balahmar, R. Mokaya, *Nat. commun.* 2017, **8**, 1545-1556.
5 E. Masika, R. Mokaya, *J. Phy. Chem. C.* 2012, ***116***, 25734-25740.
6 M. Sevilla, A. B. Fuertes, *Micropor Mesopor Mater.* 2012, **158**, 318-323.
7 M. Inagaki, M. Toyoda, T. Tsumura, *RSC Adv.* 2014, **4**, 41411-41424.
8 Z. Wang, A. Brown, K. Tan, Y. Chabal, K. Balkus, *J. Am. Chem. Soc.* 2018, **140**, 14735-14739.
9 S. B. Yoon, G. S. Chai, S. K. Kang, J. S. Yu, K. P. Gierszal, M. Jaroniec, *J. Am. Chem. Soc.* 2005, **127**, 4188-4189.
10 L. Léveillé, C. Aumaitre, J. Morin, N. Reynier, D. Larivière. *Sep. Purif. Technol.* 2019, **228**, 115709-115718.
11 D. Yuan, S. Zhang. *Sep. Purif. Technol.* **2020**, *237*. 116379-116389.
12 X. Lu, D. Zhang, A. T. Reda, C. Liu, Z. Yang, S. Guo, S. Xiao, Y. Ouyang. *Ind. Eng. Chem. Res.* 2017, ***56***, 11936-11947.
13 M. Feng, Y. Gao, D. Sarma, *J. Am. Chem. Soc.* 2018, **140**, 11133-11140.
14 Z. Dai, Y. Sun, H. Zhang, D. Ding, L. Li. *J. Chem. Eng. Data.* 2018, **64**, 4125-4225.
15 T. Di, D. Tan, Q. Yu. *Langmuir.* 2019, **35**, 13860-13871.
16 S. M. Husnain, H. Kim, *Ind. Eng. Chem. Res.* 2017, ***56***, 9821-9830.
17 F. Zhang, K. Ma, Y. Li, Q. Ran, C. Yao, C. Yang, H. Yu, S. Hu, S. Peng. *Chem. Eng. J.* 2020, **392**, 123717-123727.